Performance Trends of a Generic Small Gas Turbine Engine

Balaji Sankar and Tahzeeb Hassan Danish

Abstract Small gas turbine engines are increasingly used in cruise missile applications. In the design stage of these engines, aero-thermodynamic models are used to evaluate the expected performance of the engine for a given set of component characteristics. The throttle characteristics and altitude-Mach number characteristics of the engine are iteratively analyzed using this model. This paper describes the use of such a model to show the expected performance of a set of design choices at different altitudes and Mach numbers. These small engines are operated at maximum possible Turbine Inlet Temperatures (TIT) for maximum thrust. Theoretical relations that give the slope of the operating line for constant turbine inlet temperature operation is derived. Using these expressions, the reduction of stability at high altitude and low Mach number is shown.

Keywords Small gas turbine engine · Thermodynamic modeling

1 Introduction

Small turbo jet gas turbines are used as expendable engines for cruise missile applications. They are compact, reliable and require very little maintenance as exemplified by the Teledyne CAE J 402 engine. When designing these types of engines, the designer has to repeatedly assess the operating envelope and the performance of the designed engine. This has to be done so that the engine suits the end application, which will have a desired operating envelope, and meets thrust and SFC requirements. The designer will typically choose a compressor, turbine, and combustor geometry, which are typically derived from similar earlier engines. Aero-thermodynamic models are useful to assess the performance of the engine for the chosen compressor, combustor, and turbine characteristics. This work describes the use of such an aero-thermodynamic model to assess the performance of small gas turbines theoretically in the design stage.

B. Sankar (✉) · T. H. Danish
CSIR-NAL, Bangalore, India
e-mail: balajis_dd.thdanish@nal.res.in

C. S. Mistry et al. (eds.), *Proceedings of the National Aerospace Propulsion Conference*,
Lecture Notes in Mechanical Engineering,
https://doi.org/10.1007/978-981-15-5039-3_14

A brief description of the Harpoon missile engine is given in the next section. The modeling is done for engine specifications similar to that of this engine. Analytically, it is shown that the turbine pressure ratio does not change during off-design operation for this engine. Also for maximum speed, expendable engines such as this are at maximum turbine inlet temperatures constantly. The variation of slope of operating line with altitude and Mach number for this constant high TIT is discussed. The off-design analysis results for throttle variation at International Standard Atmosphere—Sea Level Static (ISA SLS) are presented. The trend of Specific Fuel Consumption (SFC) and thrust variation with altitude and Mach number is discussed next using the performance simulation model, Harpoon missile engine description.

2 Harpoon Missile Engine Description

The Harpoon missile is one of the most used cruise missiles employing a turbojet engine. The specifications for the engine of Harpoon missile were drawn up after extensive survey by the US government in the 1960s and the main requirement was to have long storage life and low cost of acquisition. The maintenance needs were to be reduced by bringing down the parts count of the engine. The engine also had tight diameter and length restrictions imposed by the size of the Harpoon missile. The engine had to have 99% reliability of starting after 5 years of storage and accelerate to full thrust in 5 s. The performance characteristics of J402-CA-400 engine (shown in Fig. 1) made by Teledyne (in 1972) satisfying these tight requirements are described in detail in Leyes and Fleming [1]. Teledyne decreased the cost and parts count by using investment casting for a number of parts including the airfoils and brazing together subassemblies. The lubrications system was also simplified. The front ball bearing had closed sump arrangement and rear roller bearing was grease packed. All subassemblies were run directly on the main shaft at engine RPM to reduce gearing. The fuel scheduling was done by a full authority analog engine control system for reliability. The engine has a 2 stage compression system (transonic axial + centrifugal). 20% of the main flow through the compressor passed through the NGV for cooling before entering the slinger type combustor. This not only decreased the

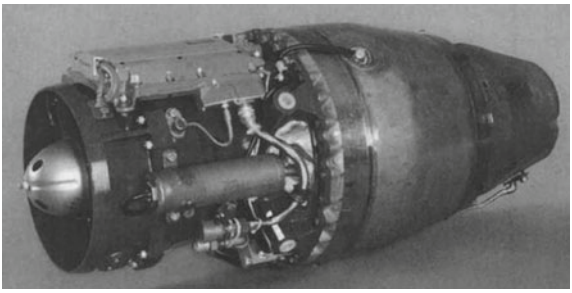

Fig. 1 Teledyne CAE J402 engine, from Leyes and Fleming [1]

heat loads on the NGV blades but also acted as pre-heater for the combustor inlet air. The engine delivers 2.93 kN thrust and weighs only 46 kgf and hence has a T/W of 6.6. The diameter of the engine was 31.7 cm and length was 74.1 cm. Since this is a missile application, the operating life is only 1 h with one time starting capability provided by a pyro-charge.

3 Engine Simulation Models

Pilidis [2] has presented the procedure to carry out digital simulations of gas turbines. Methodology to include the effect of clearances and heat soakage effects on the gas turbine performance is given. Since these effects are difficult to test individually, the results were not validated. Ismail and Bhinder [3] have presented the equations to model a turbojet performance and have given the variation of thrust and SFC with Mach number without any experimental results. As the ambient inlet temperature increased from ISA SLS by 35 °C, the power output from the engine dropped by 20%. Vivek Sanghi has given a detailed survey of the simulation techniques and their advancement over the years in Sanghi et al. [4]. NATO [5] has prepared an extensive summary of the models for engine simulation used by designers and maintainers of the gas turbines. The limits of the performance of the engine and the flight envelope of the aircraft in terms of altitude and Mach number are described in this document.

4 Analytical Thermodynamıc Model

A simplified analytical thermodynamic model is used to show the variation of turbine pressure ratio at off-design conditions and the change of slope of the operating line with altitude and Mach number. The major assumptions made to simplify the analytical model are given in the next section.

Assumptions: The major assumptions in the off-design analysis carried out here is

- Turbine entrance nozzle guide vanes and the exhaust nozzle choked to maintain constant turbine pressure ratio.
- Turbine cooling, power take-off and air take-off are not considered to maintain constant mass flow through the engine.
- Variation of γ and C_p with temperature at a particular station and fuel to air ratio are not considered to simplify the analytical expressions.

5 Π_t Change During off-Design Operation

The variation of the turbine pressure ratio over the RPM range when the engine is tested at the ground test bed is studied in this section. The mass flow rate of air as a function of total pressure and temperature is given by

$$\dot{m} = \frac{MAP}{\sqrt{T}}\sqrt{\frac{\gamma}{R}}\left(1 + \frac{\gamma - 1}{2}M^2\right)^{-\left(\frac{\gamma+1}{2(\gamma-1)}\right)}$$

In the above expression, $M =$ Mach number, $A =$ Cross section area of flow, $P =$ total pressure upstream, and $T =$ upstream total temperature. The station numbers used in this work are shown in Fig. 2. Since both the turbine and nozzles are choked ($M = 1$), mass flow through them is same and gas properties (γ, R) are assumed constant, the area ratio can be written as

$$\frac{A_4}{A_8} = \frac{P_8\sqrt{T_4}}{P_4\sqrt{T_8}} = \frac{\pi_t \pi_{\text{td}}}{\sqrt{\tau_t \tau_{\text{td}}}}$$

Simple gas turbines such as this have smooth transition duct between the turbine exit and the nozzle exit plane. The pressure drop (π_{td}) in this duct can be assumed to be constant at different flow rates and without afterburner, the temperature ratio is unity ($\tau_{\text{td}} = 1$). The choked areas of the turbine and the nozzle are also constant. Substituting for turbine pressure ratio we get

$$f(\tau_t, \eta_t) = \frac{\left(1 - \left(\frac{1-\tau_t}{\eta_t}\right)\right)^{\frac{\gamma}{\gamma-1}}}{\sqrt{\tau_t}} = \text{constant}$$

Thus if the turbine efficiency does not vary much during the off-design operation from flight idle to full speed, the turbine pressure ratio remains constant in off-design conditions also.

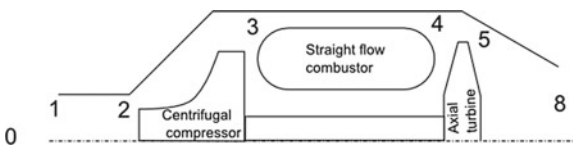

Fig. 2 Station numbering for the small gas turbine(SAE convention)

6 Operating Line Slope with Altitude and Mach Number

The operating line is essentially the variation of the compressor pressure ratio with corrected mass flow rate through the compressor. Since the turbine entry is choked, it can be used to calculate the mass flow rate through the compressor

$$\dot{m}_4 = \dot{m}_2 = \Gamma \frac{A_4 P_4}{\sqrt{T_4}}$$

where

$$\Gamma = \sqrt{\frac{\gamma}{R}} \left(\frac{\gamma + 1}{2} \right)^{-\left(\frac{\gamma+1}{2(\gamma-1)} \right)}$$

The corrected mass flow rate at the compressor inlet is given by

$$\dot{m}_c = \dot{m}_2 \frac{\sqrt{\frac{T_2}{288.15}}}{\left(\frac{P_2}{101325} \right)}$$

Substituting mass flow rate at compressor inlet using mass flow rate at turbine inlet in the expression for corrected flow rate,

$$\dot{m}_c = 5969 * \Gamma A_4 \left(\frac{P_4}{P_2} \right) \sqrt{\frac{T_2}{T_4}}$$

$$\dot{m}_c = 5969 * \Gamma A_4 \frac{(\pi_b \pi_c)}{\sqrt{\tau_b \tau_c}}$$

In the above expression, π_b and τ_b are the burner pressure and temperature ratio. π_c and τ_c are compressor pressure and temperature ratio. To change the operating point along the operating line, the turbine inlet temperature is typically controlled by the user by means of the Power Lever Angle (PLA). The ratio turbine inlet temperature to the compressor inlet temperature is given by τ_λ and ram temperature rise is given by τ_r. Writing the above equation in terms of controlled temperature ratio τ_λ, we get

$$\dot{m}_c = 5969 * \Gamma A_4 \frac{(\pi_b \pi_c)}{\sqrt{\frac{\tau_\lambda}{\tau_r}}}$$

If burner pressure loss is assumed constant, then the operating line can be expressed as

$$\pi_c = \left(\frac{\sqrt{\frac{\tau_\lambda}{\tau_r}}}{5969 * \Gamma A_4 \pi_b} \right) \dot{m}_c$$

From the above equation, it appears that the slope of the operating line depends only on the controlled temperature ratio and ram temperature ratio. This dependency can also be removed if the energy balance between the compressor and turbine is used. This energy balance can be written as

$$\tau_r \tau_c - \tau_r = \eta_{\text{mech}} (\tau_\lambda - \tau_\lambda \tau_t)$$

$$\tau_c = 1 + \eta_{\text{mech}} \left(\frac{\tau_\lambda}{\tau_r} \right) (1 - \tau_t)$$

$$\left(\frac{\tau_\lambda}{\tau_r} \right) = \frac{1}{\eta_{\text{mech}}} \left(\frac{\tau_c - 1}{1 - \tau_t} \right)$$

Substituting this in the expression for the operating line,

$$\pi_c = \left(\frac{\sqrt{\frac{1}{\eta_{\text{mech}}} \left(\frac{\tau_c - 1}{1 - \tau_t} \right)}}{5969 * \Gamma A_4 \pi_b} \right) \dot{m}_c$$

In the above expression, the compressor temperature ratio still depends on the compressor pressure ratio through the compressor efficiency ($\tau_c = f(\pi_c, \eta_c)$). For constant transition duct pressure loss and turbine efficiency, it has been shown earlier that the turbine temperature ratio and pressure ratio are constant (τ_t = constant). Hence, the slope of the operating line is constant for a given turbine inlet area (A_4) and burner pressure drop (π_b). It does not change with ambient conditions or Mach number of flight.

6.1 Reason for Increasing Stability Margin at High Mach Numbers for Expendable Engines

In expendable small gas turbines, the turbine inlet temperature is maintained constant at the max safe limit at all operational altitudes to get maximum thrust. At constant Turbine Inlet Temperature (TIT), the operating line shifts to the left toward surge with increase in altitude and shifts right away from surge with increase in Mach number.

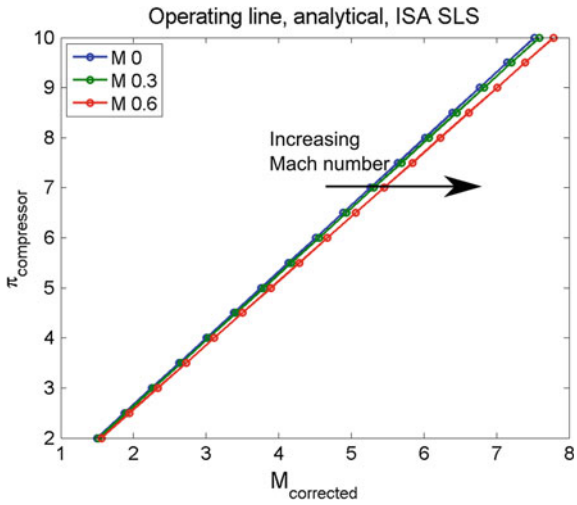

Fig. 3 Compressor operating line shifting to the right with increase in mach number at constant turbine inlet temperature

This is because, at constant TIT, the mass flow through the engine increases as Mach number increases. If τ_λ was kept constant, the TIT would have increased with increase in ram air temperature as the density at choke point would have reduced. But since TIT is kept constant and not τ_λ, the density does not decrease in relation with increase in ram air temperature. So the mass flow increases, and the surge margin increases for a given pressure ratio. This trend is shown in Fig. 3. For similar reason, increase in altitude decreases the mass flow through the engine as the fixed TIT does not allow the density at the turbine inlet to increase. Hence mass flow through the engine decreases and operating line moves toward the surge as shown in Fig. 4. So surge margin decreases with increase in altitude.

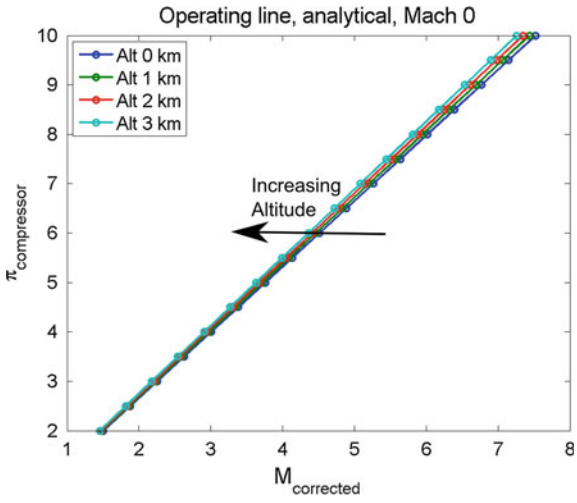

Fig. 4 Compressor operating line shifting to the left with increase in altitude at constant turbine inlet temperature

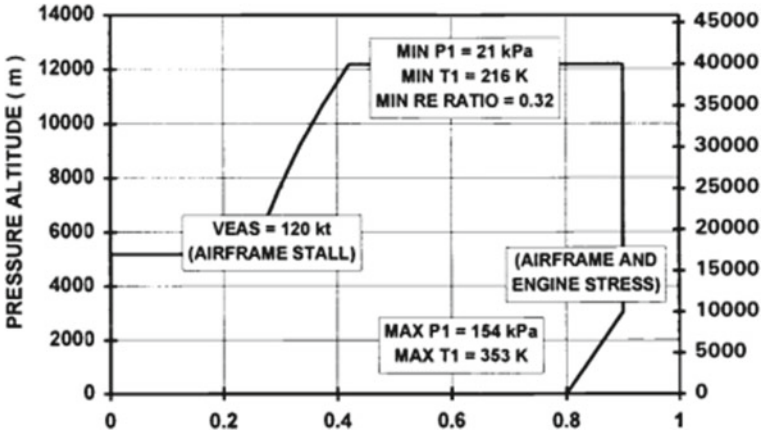

Fig. 5 Operational envelope for a subsonic air-breathing missile, from Walsh [6]

For these two reasons, the upper left corner of the flight envelope, where the engine encounters high altitude, low Mach number, is susceptible to surge of the gas turbine. This region of operation is avoided as shown in Fig. 5.

7 Design Point Specifications

The small gas turbine (turbojet) engine without afterburner has been thermodynamically analyzed theoretically for its design point performance. Figure 2 shows the configuration and stations of the engine. The engine comprises a centrifugal compressor, straight flow combustor, axial turbine, and convergent fixed area nozzle. For simplicity of analysis, turbine nozzle guide vanes and nozzle are assumed to be choked, power off-take and turbine cooling are not considered, fuel-air ratio is assumed very small, and specific heat capacity and specific heat ratio of the air at a particular station is assumed constant. The design point parameters of the engine are given in Table 1. The thrust and SFC of the engine at design point are 3.1 kN and 0.116 kg/N-h.

Table 1 Design point parameters of the turbojet engine

Parameter	Value
Compressor pressure ratio	6
Compressor efficiency	0.79
Turbine efficiency	0.9
Design Mass flow rate, kg/s	5
Burner efficiency	0.97
Design fuel flow rate, kg/s	0.101
Turbine inlet temperature, K	1220
Burner pressure ratio	0.94
Nozzle pressure ratio	0.98
Discharge coefficient of nozzle	0.98
Thrust coefficient of nozzle	0.98
Leakage flow, kg/s	0.01
Inlet pressure recovery	0.95
Compressor exit pressure drop	0.98
Mechanical efficiency	0.99

8 Off-Design Performance Analysis

Off-design performance analysis mainly consists of two parts. First is the throttle characteristics, which the response of the engine to variation in N1 RPM at a fixed ISA SLS condition. Second is the variation of performance at various altitudes and Mach number combinations. In altitude-Mach characteristics, typically, the analysis is carried out to find the maximum possible thrust at each altitude and Mach number. This determines the maximum possible acceleration of the vehicle from this condition. Both throttle analysis and altitude-Mach characteristics require component characteristics maps. The normalized compressor characteristics, turbine, and nozzle characteristics map used in this work are shown in Figs. 6 and 7. The methodology of off-design simulation is given in detail in Walsh and Fletcher [6], Cohen et al. [7], Cumpsty [8], and Mattingly [9]. The authors have used similar off-design modeling programs using Matlab for the performance analysis of legacy aircraft engines as reported in and is not repeated here.

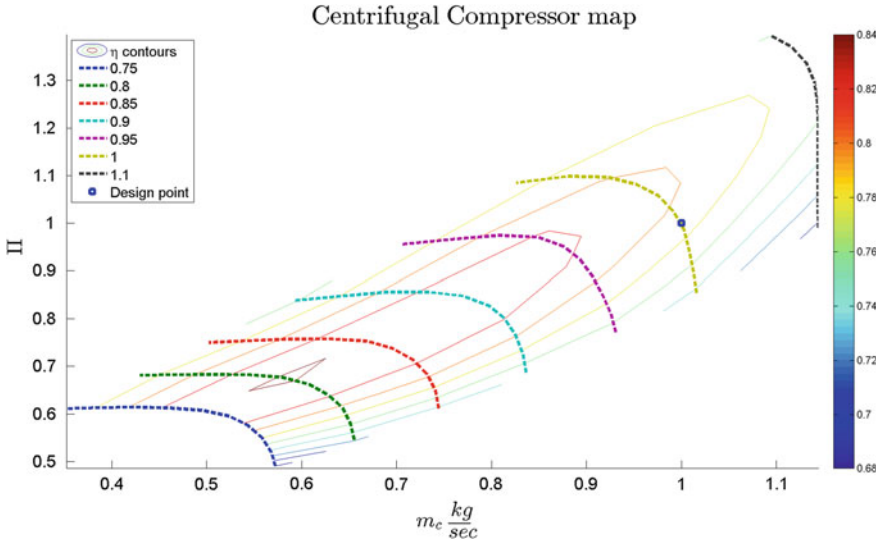

Fig. 6 Compressor characteristics map showing with normalized mass flow rate and pressure ratio

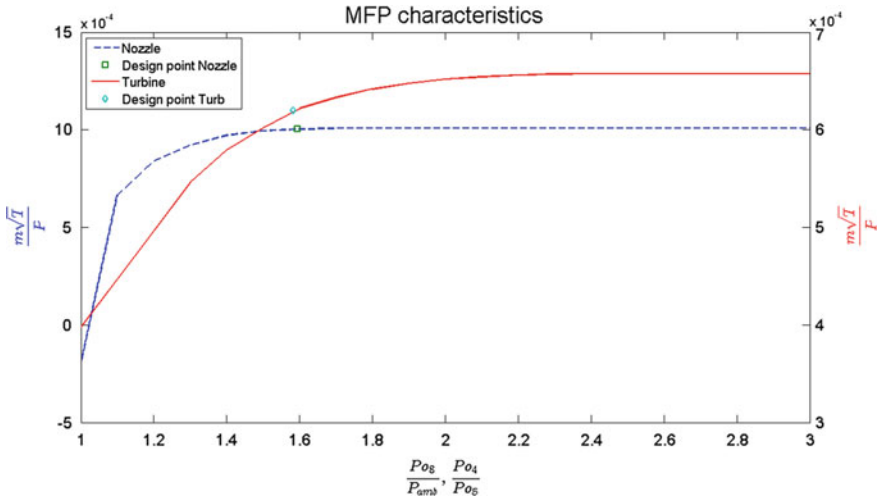

Fig. 7 Convergent nozzle characteristics map showing mass flow function dependence on pressure ratio

8.1 Results of Throttle Characteristics Simulation at ISA SLS

The performance of the engine in terms of thrust and fuel consumption at ISA SLS for various RPM is shown in Figs. 8 and 9. The values are normalized using design point values. From Fig. 8 we can infer that the nozzle chokes above 90% RPM and the engine generates pressure thrust, which increases the total thrust of the engine.

Fuel to air ratio variation and turbine corrected RPM ($N1T_c$) variation are shown in Fig. 10. The turbine corrected RPM (shown in green) increases and is maximum at 85% $N1_c$ due to the variation of burner exit temperature (TIT) with RPM. The variation of TIT (shown in Fig. 11) is almost parabolic with respect to RPM and a corresponding parabolic trend is seen in $N1T_c$. The trend of variation of fuel to air ratio also follows the trend of variation in TIT. Pressure variation, which is similar to the temperature variation, is shown in Fig. 12.

The operating line of the engine on the compressor map is shown in Fig. 13. We can see that the operating line becomes steeper as the RPM increase. As expected for a single spool engine, the surge margin of the compressor is high at low RPM and low at high RPM. The engine is more susceptible to surge at as the RPM increases above design RPM.

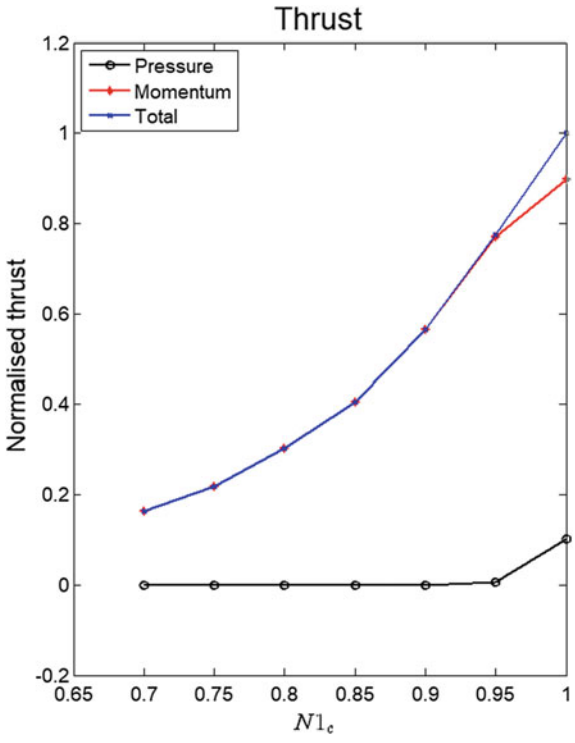

Fig. 8 Thrust variation at ISA SLS for various RPM

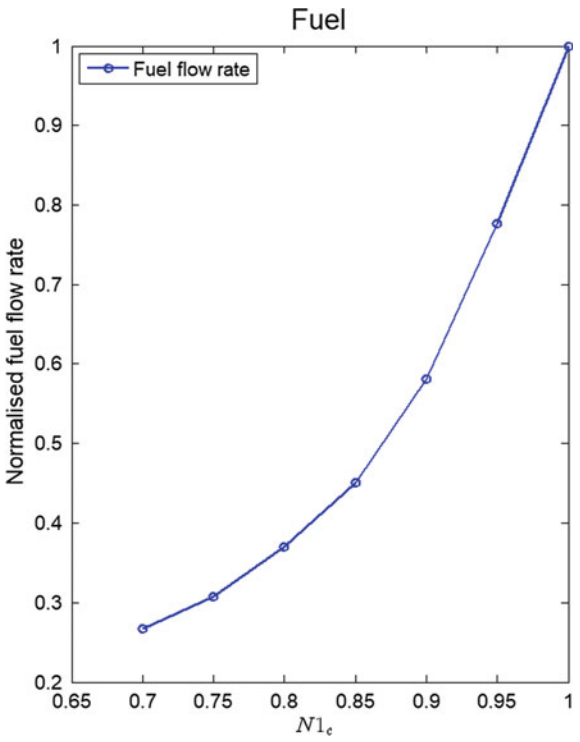

Fig. 9 Fuel flow rate variation at different stations at various RPM

The operating point of the engine on the turbine and nozzle Mass Flow Parameter (MFP) curves is shown in Fig. 14. Design point of the engine lies in the region where both the turbine and nozzle are choked and MFP is constant. As the RPM reduces, the pressure ratio across both the components drops and the mass flow parameter reduces. This forces the engine to ingest lower mass flow at lower RPM.

8.2 Results of Altitude-Mach Characteristics off-Design Simulation

Typical variation of peak thrust with Mach number at different altitudes for a turbojet engine is shown in Fig. 15. It can be seen that at sea level, initially thrust drops due to inlet air momentum increase. It again rises beyond Mach 0.5 due to ram pressure rise. Similar trend in thrust can be seen in the contour plot as shown in Fig. 16.

The change in N1c RPM is shown in Fig. 17. At high altitudes and low Mach number, inlet temperature is low and velocity of sound is hence low. Thus N1c is high at top left corner of the envelope. Since compressors have a limitation on maximum N1c due to shock losses, the gas turbine may not operate satisfactorily in this region.

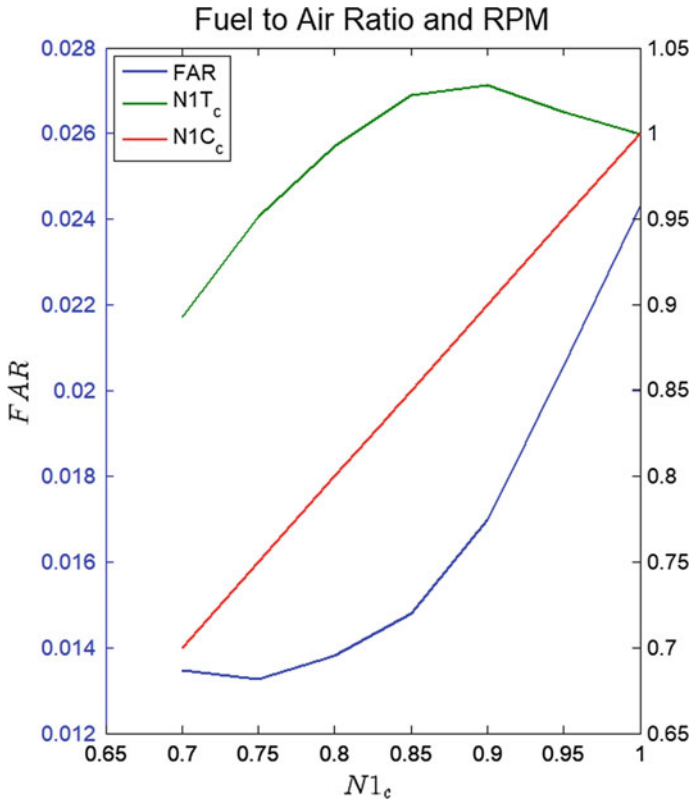

Fig. 10 Fuel to air ratio and turbine corrected RPM variation at different stations at various RPM

When this high RPM region of operation is removed from thrust characteristics, the resulting contour plot is shown in (Fig. 17) Fig. 18.

When the RPM is held constant at 100%, the TIT drops below design value at the lower right corner of the envelope (Fig. 19). This is because, at low altitude and high Mach numbers, the mass flow rate into the engine increases. To keep MFP constant, the TIT has to be reduced. For the same reason, TIT increases at low Mach number high altitude conditions. Since there are material limitations on the TIT values for uncooled turbines, the engine cannot be operated in these high TIT regimes. When this high TIT region of operation is removed from thrust characteristics, the resulting contour plot is shown in Fig. 20.

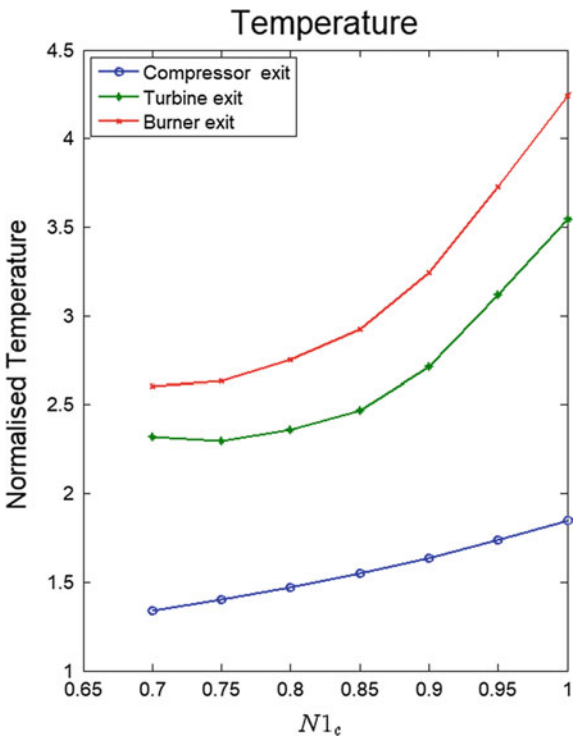

Fig. 11 Temperature variation at different stations at various RPM (Normalized using ISA SLS temperature)

8.3 SFC Variation with Altitude and Mach Number

Typical variation of SFC with Mach number at different altitudes for a turbojet engine is shown in Fig. 21. It can be seen that at all altitudes, SFC increases with Mach number. At higher altitudes, SFC of the engine reduces for the same Mach number. Similar trend can be seen in the SFC contour plot shown in Fig. 22.

9 Conclusions

The performance analysis of a generic turbojet engine was carried out using an aero-thermodynamic model in this work. Design point and off-design analysis (throttle and altitude-Mach characteristics) were carried out. Performance trends obtained in altitude-Mach characteristics were similar to published trends in literature. The reason for not operating in high altitude and low Mach number combination was shown from both high N1c and high TIT points of view. Also it was shown analytically

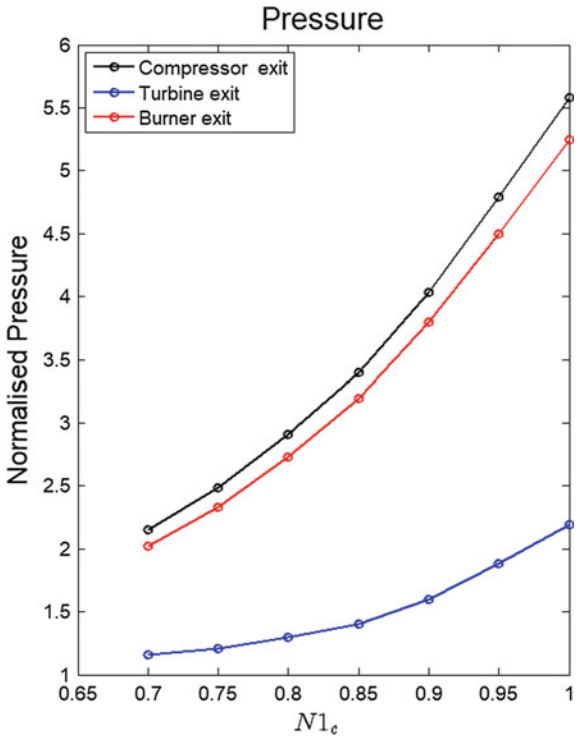

Fig. 12 Pressure variation at different stations at various RPM

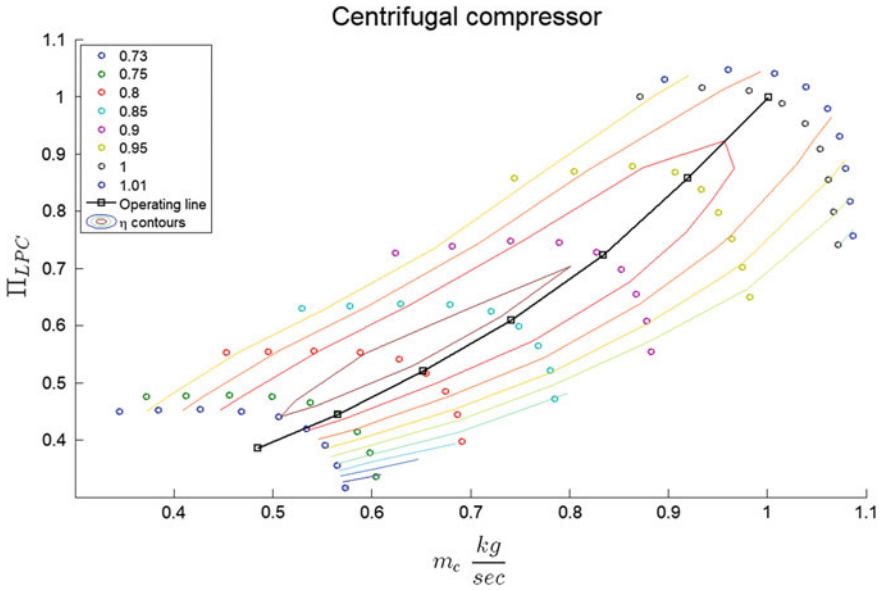

Fig. 13 Normalized compressor map with operating line during throttle input variation

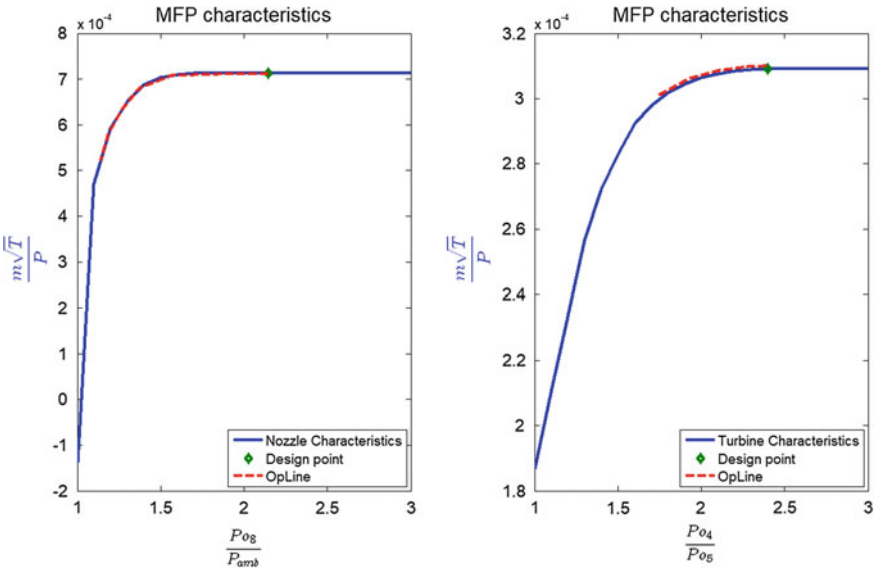

Fig. 14 Turbine and nozzle mass flow parameter curves with operating line during throttle input variation

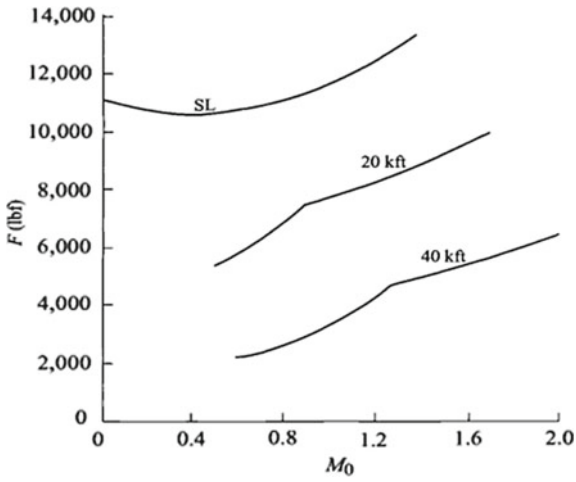

Fig. 15 Variation of thrust at 100% RPM with Mach number at different altitudes, from Mattingly [9]

that the slope of the operating line increases at high altitude and low Mach number for constant TIT operation. This increasing operating line slope decreases the surge margin available.

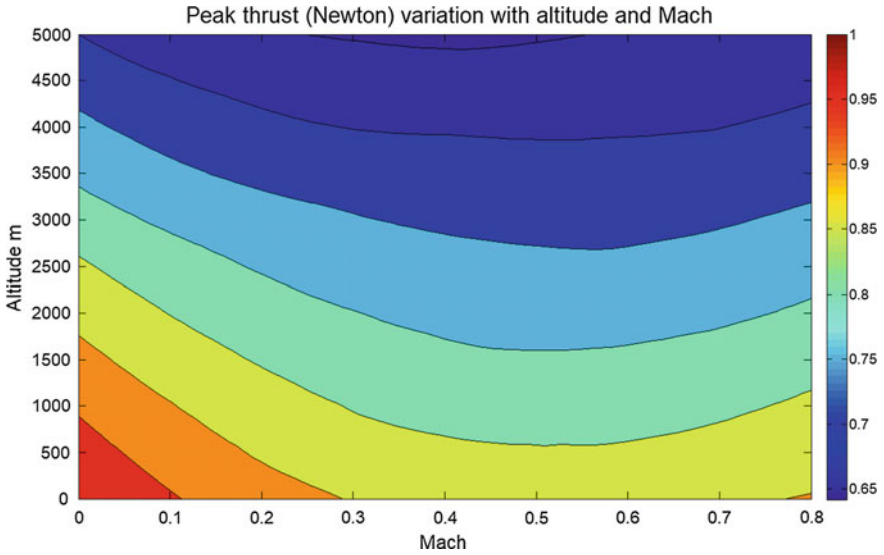

Fig. 16 Variation of peak thrust with altitude and Mach number at constant 100% physical engine RPM

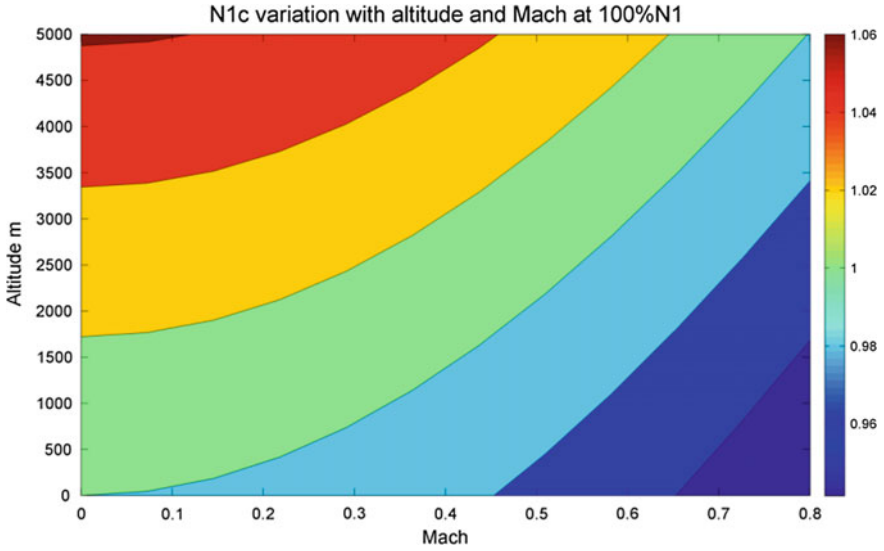

Fig. 17 Variation of corrected engine RPM with altitude and Mach number at constant 100% physical engine RPM

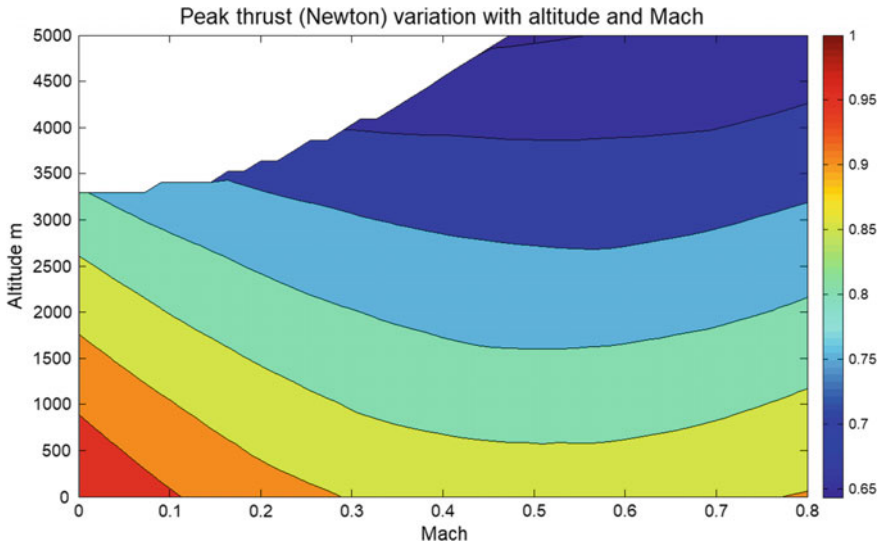

Fig. 18 Variation of thrust at 100% RPM with altitude and Mach number at constant 100% physical engine RPM. N1c has been limited to 1.04

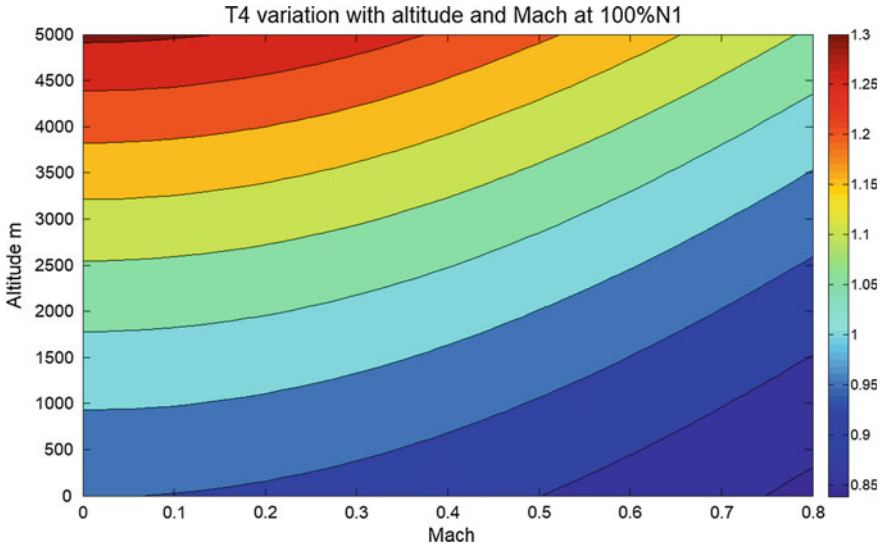

Fig. 19 Variation of combustor exit temperature with altitude and Mach number at constant 100% physical engine RPM

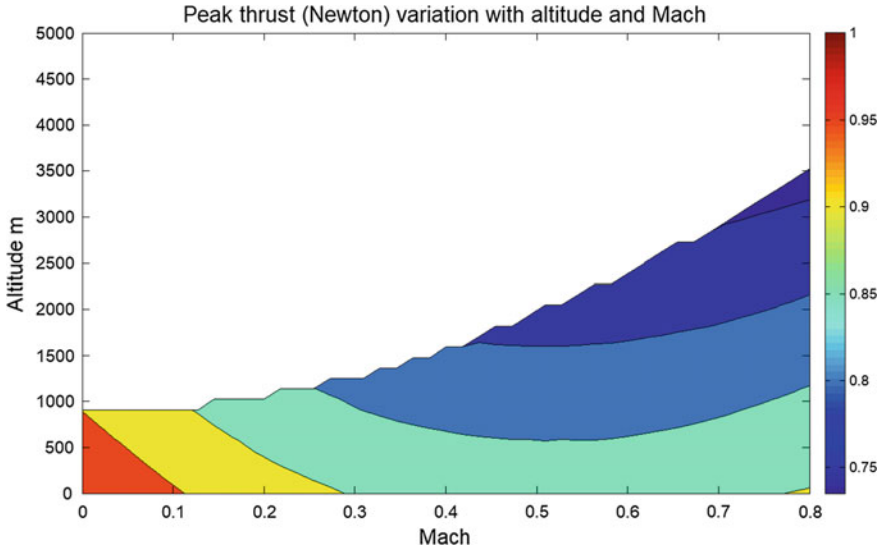

Fig. 20 Variation of thrust at 100% RPM with altitude and Mach number at constant 100% physical engine RPM. TIT has been limited to 1220 K

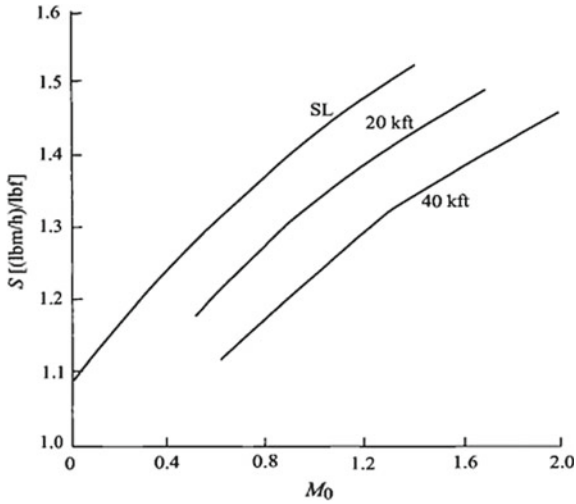

Fig. 21 Variation of SFC at 100% RPM with Mach number at different altitudes., from Mattingly [9]

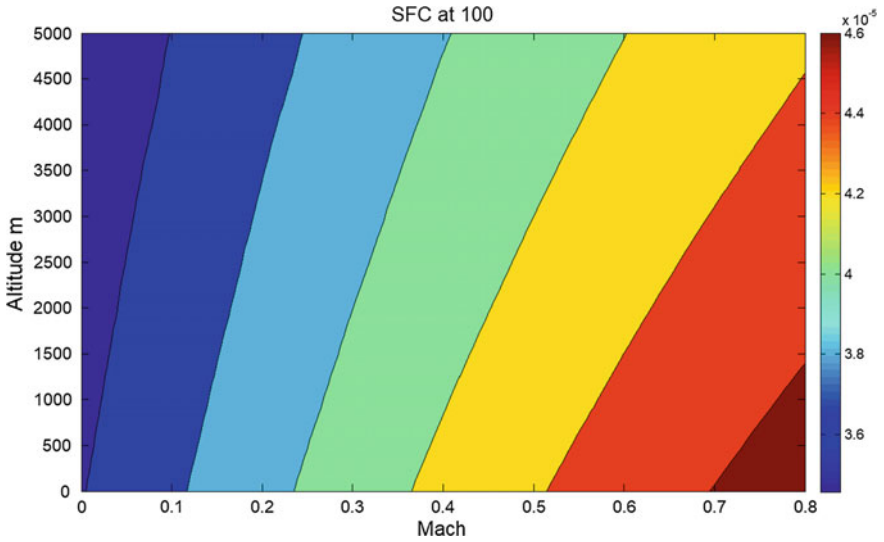

Fig. 22 Variation of SFC at 100% RPM with altitude and Mach number

References

1. Leyes RA, Fleming WA (1999) The History of North American Small Gas Turbine Aircraft Engines. AIAA
2. Pilidis P (1983) Digital simulation of gas turbine performance, Doctoral dissertation. University of Glasgow
3. Ismail IH, Bhinder FS (1990) Simulation of aircraft gas turbine engines. In: ASME 1990 international gas turbine and aeroengine congress and exposition. American Society of Mechanical Engineers, pp V002T02A033–V002T02A033
4. Sanghi V, Lakshmanan BK, Sundararajan V (2000) Survey of advancements in jet-engine thermodynamic simulation. J Propul Power 16(5):797–807
5. NATO (2002) Performance prediction and simulation of gas turbine engine operation, RTO TR-044/AVT-018
6. Walsh PP, and Fletcher P (2004) Gas turbine performance, 2nd edn. Blackwell science, Oxford
7. Cohen H, Rogers GFC, Saravanamuttoo HIH (1996) Gas turbine theory, 4th edn. Longman House, Essex
8. Cumpsty N (2003) Jet propulsion. United Kingdom at the University Press, Cambridge, Cambridge University Press
9. Mattingly, JD (2006) Elements of propulsion: gas turbines and rockets. AIAA Education series, Blacksburg, Virginia